

RESEARCH PAPER

## Silver nanoparticles synthesized with a fraction from the bark of *Eysenhardtia polystachya* with high chalcone and dihydrochalcone content effectively inhibit oxidative stress in the zebrafish embryo model

Abraham Heriberto Garcia Campoy<sup>1</sup>, Fernando Felipe Martinez Jeronimo<sup>2\*</sup>, Rosa Martha Perez-Gutierrez<sup>1</sup>, Alethia Muñiz Ramirez<sup>3</sup>

<sup>1</sup>Laboratorio de Investigación de Productos Naturales. Escuela Superior de Ingeniería Química e Industrias Extractivas IPN. Av. Instituto Politécnico Nacional S/N, Unidad Profesional Adolfo Lopez Mateos CP 07708, Cd. Mexico

<sup>2</sup>Lab. De Hidrobiología Experimental. Escuela Nacional de Ciencias Biológicas. Carpio y Plan de Ayala S/N, Cd de México. CP 11340

<sup>3</sup> CONACYT-IPICYT / CIIDZA, Camino a la Presa de San Jose 2055, Col. Lomas 4 section, CP 78216 San Luis Potosí México

### ABSTRACT

**Objective(s):** In this study, we describe a simple eco-friendly approach for the synthesis of a potent, stable and benign silver nanoparticles to carry and deliver chalcones and dihydrochalcones present in a methanol extract of *Eysenhardtia polystachya* (EP).

**Materials and Methods:** In this process silver nanoparticles carrying EP compounds (EP/AgNPs) are synthesized in a single step by eliminating the additional handling associated with incorporating EP compounds. The resulting nanoparticles (EP/AgNPs) were characterized using several physicochemical techniques. Cell viability was measured in vitro with RAW264.7 murine macrophage cells. In addition, we evaluated the ability of EP and EP/AgNPs to protect against glucose-induced oxidative in vivo stress using zebrafish embryos.

**Results:** The synthesized EP/AgNPs showed an absorption peak at 413 nm on ultraviolet-visible spectroscopy (UV-vis), revealing the surface plasmon resonance of the nanoparticles. Transmission electron microscopy (TEM) indicated that most of the particles were spherical with a diameter of 10 to 12 nm, a polydispersity index (PDI) of 0.197 and a zeta potential of -32.25 mV, suggesting high stability of these nanoparticles. This study also demonstrated the biocompatibility of the nanoparticles when tested in RAW264.7 cells and its protective efficacy against oxidative stress induced by the exposure of zebrafish embryos to high glucose concentrations. Treatment with EP/AgNPs increased the activity of anti-stress biomarkers such as superoxide dismutase (SOD), catalase (CAT), glutathione peroxidase (GPx), and total soluble protein. Exposure of the embryos to EP/AgNPs significantly ( $P < 0.05$ ) suppressed the formation of malondialdehyde (MDA) and lipid oxidation (LPO).

**Conclusion:** EP/AgNPs synthesized from *E. polystachya* extract provide an effective defense against oxidative stress in zebrafish embryos.

**Keyword:** chalcones, dihydrochalcones, *Eysenhardtia polystachya*, oxidative stress, silver nanoparticles, zebrafish

### How to cite this article

Heriberto Garcia Campoy A, Felipe Martinez Jeronimo F, Martha Perez-Gutierrez R, Muñiz Ramirez A. Silver nanoparticles synthesized with a fraction from the bark of *Eysenhardtia polystachya* with high chalcone and dihydrochalcone content effectively inhibit oxidative stress in the zebrafish embryo model. *Nanomed J.* 2018; 5(3): 152-162. DOI:10.22038/nmj.2018.005.0005

### INTRODUCTION

Reactive oxygen species (ROS) are produced during normal metabolism and are generated in

cells as a response to various factors including ionizing radiation, chemical agents, ultraviolet light, and thermal oxidative stress. ROS play a dual role in biological systems: by being either beneficial or harmful [1]. ROS generate cellular responses, including the activation of numerous

\* Corresponding Author Email: [rmpg@prodigy.net.mx](mailto:rmpg@prodigy.net.mx)

Note. This manuscript was submitted on May 1, 2018; approved on June 15, 2018

cellular signaling systems, and act as a defense against infectious agents [1]. However, at high concentrations, ROS can induce oxidative stress, producing severe intracellular damage that can lead to cell death, and they are elevated in various pathological conditions and diseases including atherosclerosis, age-related disorders, diabetes, rheumatoid arthritis, cancer, inflammatory diseases and neurodegenerative disease [2]. In the presence of transition metal ions, ROS cause lipid peroxidation, an oxidative deterioration of polyunsaturated lipids that produces cytotoxic products, mainly aldehydes such as 4-hydroxynonenal (HNE) and malondialdehyde (MDA) [3]. Under some circumstances, the antioxidant enzyme defense system can maintain cellular homeostasis and oxidative balance to protect cells from oxidative stress and restore antioxidant activity [4]. In addition, organisms possess antioxidant enzymes as glutathione peroxidase (GPx), reduced glutathione (GSH), catalase (CAT) and superoxide dismutase (SOD) that prevent the harmful effects of ROS [4].

Nanoceria has been studied extensively in human cell lines and animal models as a means to restore oxidant/antioxidant imbalance and defend cells against oxidative stress [5]. Nanoparticle size metals and dispersed particles are part of nanotechnology developments; among them silver nanoparticles are the most intensively studied in the field of green synthesis of nanomaterials because AgNPs are of great interest due to their unique biological, chemical and physical characteristics [6]. Among its physical-chemical properties as ease of synthesis, broad optical properties, and surface functionalization offer new opportunities for the therapy of cancer [7], antimicrobial use [8] and drug delivery [9].

Several methods for the preparation of silver nanoparticles have been reported. They include thermal evaporation as silver aerosol [10], reduction of silver in fatty acid film [11], chemical reduction of silver without stabilizer [12], silver sol preparations by chemical and photo-reduction [13]. Biosynthesis processes through the use of a plant extract as a reducing agent [14]. The enriched source of plant extracts has a considerable attention for nanoparticles biosynthesis, because phenolic compounds act as stabilizing, capping agent and reducing agents, which leads to colloidal nanoparticles. The *Portulaca oleracea* extract form nanoparticles of different sizes; 175 nm 146 nm,

and 136 nm, from stem, leave, and root extracts, respectively [15], authors in this study support that the size of the particle depends of the reducing agent, consequently we used sodium borohydride (NaBH<sub>4</sub>) as reducing agent in an attempt to obtain nanoparticles of smaller size to improve their effectiveness against oxidative stress.

Other examples are the extract of flowers of *Bauhinia variegata* used for the biosynthesis of AgNPs covered with anthocyanins such as peonidin-3-diglucoside, malvidin-3-glucoside, malvidin-3-diglucoside and cyanidin-3-glucoside [16]. These compounds protect against DNA cleavage, oxidant and have inflammatory effects [17]. *Ambrosia maritima* biosynthesized silver nanoparticles has also antioxidant and antimicrobial properties [18].

The main mechanisms toxicity is through ROS generation, causing oxidative stress and producing damage to cellular components and to the cell membrane, Ag<sup>+</sup> ions bind to proteins, causing inactivation, in addition, promote disabling of proteins, depletion of antioxidant molecules, activation of antioxidant enzymes and DNA damage [19]. Nevertheless, some molecules contained in plants significantly reduce the toxicity of AgNPs due to the chemical nature of the surface coating.

The zebrafish experimental animal model (*Danio rerio*) is widely used for *in vivo* experiments for its similarity to human genetically in biology, pharmacological and toxicological studies of drugs, contaminants and new compounds especially in mechanism determination [20].

*Eisenhardtia polystachya* (Ortega) Sarg (kidney wood), belongs to the Fabaceae family, is a tree found in subtropical and tropical regions in Latin America including Mexico. Traditionally has been used for the treatment of bladder disorders, antidiabetic, antirheumatic and against nephrolithiasis [21]. Bark contain polyphenols [22] such as isoflavans with a moderate effect against KB cell lines [23], flavonoids reducing oxidative stress in streptozotocin-induced diabetes in mice [24] and dihydrochalcones reducing the formation of AGEs [25]. Various studies showed that a methanol-water extract possess antidiabetic activity, inhibit the glycation of proteins (AGEs), and antioxidant potential [26].

Currently, there are no reports studies on silver nanoparticles from *E. polystachya* neither for its use as a delivery system for *E. polystachya* extracts

or for its use, against chronic and degenerative diseases.

Taking into account the multiple advantages of the zebra fish model, we chose it to determine the protective effect of EP and EP-AgNPs against glucose-induced oxidative stress by evaluating the levels of LPO, total protein, SOD, CAT and GPx in treated and untreated animals.

## METHODS

### Chemicals

Acetonitrile, acetic acid, dimethylsulfoxide (DMSO), 3-(4,5-dimethylthiazol-2-yl)-2,5-diphenyltetrazolium bromide (MTT), 2,2-diphenyl-1-picrylhydrazyl (DPPH), dithiothreitol (DTT), Dulbecco's modified, Eagle's medium (DMEM), glibenclamide (GB), fetal bovine serum (FBS), glucose, glutamine, methanol, phosphate buffered saline (PBS), polyvinyl pyrrolidone (PVP), silver nitrate ( $\text{AgNO}_3$ ), sodium borohydride ( $\text{NaBH}_4$ ), thiobarbituric acid (TBA), trichloroacetic acid (TCA) were used in this study. All chemicals were reagent grade, purchased from Sigma-Aldrich (St. Louis, MO, USA).

### Plant materials

*E. polystachya* Bark was collected in the Mexican state of Hidalgo in October 2016 near the city of Tula. A voucher specimen (No. 49584) was taxonomical identity by the specialist Prof. Aurora Chimal, and was deposited in the Herbarium of Universidad Autonoma Metropolitana-Xochimilco, Mexico.

### Preparation of bark extract (EP)

Bark of *E. polystachya* (1 kg) was dried and ground which was extracted with ultrapure water (MilliQ water) and methanol (laboratory reagent) (3 X 3 L) for 5 days [27]. The extracted water/methanol was filtered and evaporated under vacuum at 40 °C, the yield of the crude extract was 95 g which was kept in the desiccator. The bark extract of *E. polystachya* (EP) was prepared by dissolving in MilliQ water.

### Synthesis of EP/AgNPs

Briefly, 0.03 moles of silver nitrate ( $\text{AgNO}_3$ ) was dissolved in 50 mL of MilliQ water. The silver nanoparticles (Ag-NPs) were synthesized in dark conditions beneath constant stirring with a magnetic stirrer. Then, in an ice bath 30 mL of sodium borohydride ( $\text{NaBH}_4$ ) 0.002 M solution was

added dropwise and mixed well. After the reaction mixture is added 10 mL of a solution of EP. The presence of grayish-brown colour suggested the formation of EP/AgNPs. To prevent aggregation was added 30 mL of polyvinyl pyrrolidone (PVP) 0.3% solution. After, EP/Ag NPs were collected by centrifugation for 30 min at 15,000 rpm. Then, washing the EP/AgNPs two times with MilliQ water the excess of silver ions was removed followed by centrifugation for 30 min at 1000 rpm. Ag-NPs without EP were synthesized using the same method which was used as control [28]. After the synthesis was authenticated by UV-Vis spectroscopy of colloidal solution of EP/AgNPs.

### Characterization of EP/AgNPs

EP/AgNPs, were characterized using UV-Vis spectrophotometer (UV-1800, Shimadzu, Kyoto, Japan), fourier transformed infrared spectroscopy (FT-IR) using a Perkin-Elmer spectroscope (L1280044, Waltham, MA, USA), TEM using an H-600 instrument (Hitachi, Japan), Malvern Zetasizer Nano ZS90 compact scattering spectrometer (Malvern Instruments Ltd., Malvern, UK) and Nicomp 380 particle size analyzer (Nicomp Particle Sizing Systems, Port Richey, FL, USA). in order to identify functional group, structure, shape, size and hydrodynamic diameter of the nanoparticles [29].

### Encapsulation efficiency (EE) and EP loading content (Dlc)

The amount of EP loaded was measured by addition of 20 mg of nanoparticles in 50 mL of MilliQ water. EE and Dlc of EP/AgNPs were estimated by extracting EP from the nanoparticles by calculating the difference between the initial amount of EP used in the synthesis and the amount of EP contained in supernatant after centrifugation for 15 min at 14,000 rpm. The supernatant was assayed by UV-Vis spectrophotometry at 328 nm in nanoparticles synthesized without EP was used the same procedure. Equations 1 and 2 were used to calculate the EE and Dlc [30]:

$$\% EE = (\text{weight of EP in nanoparticles} - \text{Free EP in the nanoparticles}) \times 100 \quad (1)$$

Total amount of EP

$$\% Dlc = (\text{weight of EP in NP} / \text{weight of NP}) \times 100 \quad (2)$$

### Stability of EP-loaded AgNPs nanoparticles in aqueous solution

The stability of EP/AgNPs was determined,

during 6 months room storage by measuring the absorbance at 328 nm which was compared with a freshly prepared EP/AgNPs. After this time nanoparticles did not show aggregation [31].

#### **Dynamic antioxidant capability Test**

EP/AgNPs (0.1 g) were diluted in 1 liter of MilliQ water at pH 6.0. Then, 1.9 mL of a solution 0.1M 2,2-diphenyl-1-picrylhydrazyl (DPPH·) in methanol was added to 100 µL of this solution and incubated at room temperature for 10, 20, 30, 40, 50, 60 and 70 h 45 min in the dark. After, the absorbance was measured at 517 nm [32]. Scavenging activity was calculated using the following formula:

$$\text{DPPH radical scavenging effect (\%)} = [(A_0 - A_1)/A_0] \times 100 \quad (1)$$

Where  $A_0$  was the absorbance of control and  $A_1$  was the absorbance of the sample

#### **In vitro EP release**

For in vitro release detection, 10 mg of EP/AgNPs were suspended in 10 mL of PBS with pH 1.2 simulating the gastric fluid (SGF), and at pH 6.6, 7.0 and 7.4 simulating intestinal fluid (SIF) with constant stirring with a magnetic stirrer at 37 °C. At different intervals, aliquots were taken and centrifuged at 8000 rpm. Further, contained of EP by measuring the absorbance at 328 nm. To determine the EP release mechanism, the data were fitted to the Korsmeyer-Peppas model [33].  $M_t/M_\infty = Kt^n$ , In this equation,  $M_t$  and  $M_\infty$  are the absolute amounts of EP released at time  $t$  and at infinite time, respectively,  $K$  is a constant related to the structural characteristics of the particles, and  $n$  is the release exponent reflecting the diffusion mechanism.

#### **Cell cultures**

RAW264.7 macrophages were purchased from the American Type Culture Collection (Rockville, MD, USA) and were cultured in Dulbecco's modified Eagle's medium (DMEM) supplemented with 100 µg/mL of streptomycin, 100 units/mL of penicillin and 10% fetal bovine serum (FBS). RAW264.7 cells were maintained in a humidified atmosphere with 5% CO<sub>2</sub> at 37 °C. EP was dissolved in DMSO.

#### **Cell viability test**

To evaluate cell viability, RAW264.7 cells were cultured in 96-well plates in Dulbecco's modified Eagle's medium (DMEM) supplemented with 10% FBS. Macrophages were treated with different concentrations of EP/AgPNs (140, 280, 420

and 560 µg/mL) and incubated for 1 h. After incubation period, 20 ng/mL lipopolysaccharide (LPS) was added to each well and incubated at 37 °C for 4 h and 5% CO<sub>2</sub>. Further, the cells were treated with 0.5 mg/mL of MTT and incubated overnight. The index cell viability was measured with a microplate reader at an absorbance of 570 nm [34]. Cell viability was evaluated relative to the untreated control macrophages.

#### **Experiments on zebrafish embryos model**

Specimens of *Danio rerio* of both sexes were acclimatized to laboratory conditions for a period of 15 days before start the experimentation. During the adaptation period, fish were fed once daily with brine shrimp (*Artemia nauplii*). One third of water was replaced 1 h after feeding to remove excreted wastes. Adult zebrafish were maintained at  $27.4 \pm 0.58$  °C in a flow-thru system in a 14:10-h light: dark cycle. After postfertilization (hpf) the embryos were collected randomly and select those that had a developed normally under a stereomicroscope and incubated in dishes (250 embryos per dish). Larvae and embryos were kept in Ringers solution at pH 7 throughout the experiment. All animal procedures were approved by the Institutional Ethical and complied with international guidelines.

#### **Oxidative stress induction**

Because embryos exhibit a weak antioxidant defense capacity during the first stages of organogenesis, their sensitivity to the tested substances is increased. Zebrafish were maintained in groups of 6-8 larvae/well in 24 well plates with daily exchanges of solutions to prevent microbial growth. Zebrafish embryos were exposed for 24 h (i.e., from 24– 48 hpf) to a glucose concentration of 25 mM/L in water (Deer Park) in 24 well plates. Except for the glucose stock solution, the water used is the same as that used for culture and maintenance of *D. rerio* adults.

When stress was observed, the embryos were placed in a recovery tank without glucose solution. If the embryos showed no signs of distress during the first four hours, they were kept overnight in the glucose solution [36]. Control animals were maintained in aquariums with stock aquarium water for the same period in the absence of glucose.

#### **Effect of EP and EP/AgNPs on oxidative stress in zebrafish embryos**

After exposure to glucose, the zebrafish

embryos/larvae were evaluated for specific toxicity endpoints, including body length, survival rate and morphological abnormalities. To evaluate the ability of EP and EP/AgNPs to protect against glucose-induced oxidative stress, glucose-treated embryos were incubated for 96 h with various concentrations of EP/AgNPs (25, 50, 100 and 200 mg/mL), with 200 mg/mL of the extract (EP) or with the reference drug: 5 mg/mL glibenclamide for 14 days. After, finishing the exposure periods the fishes were prepared in proportion of 1 g tissue per 10 volumes of buffer (0.1M Tris-EDTA buffer, pH 7.4) in ice-cold using a homogenizer at 10,000 rpm for 15 min at 48 °C. Supernatants collected were used to evaluate the biochemical parameters and protein appraisal.

### Biochemical parameters

The supernatant was used directly in this study. The formation of SOD, CAT, and GPx activities were measured using commercial kits acquired from Cayman Chemical (Ann Arbor, MI, USA) and used according to the manufacturer's instructions. The protein concentration was evaluated by the Bradford [37] as described in the Bio-Rad protein assay kit (Thermo Fisher Scientific, Waltham, MA, USA). Control animals were kept in the same conditions as the treated groups but in the absence of glucose. Glibenclamide (GB) was used as a standard.

### Determination of lipid peroxidation (LPO)

Briefly, 100 µL of the tissue homogenate was added to 0.15 mL of 10 mmol KH<sub>2</sub>PO<sub>4</sub> and 0.5 mL TrisHCl buffer (pH 7.4) and 0.25 mL of distilled water. The tubes were incubated at 37 °C for 20 min with soft shaking. Then, was added 1 mL of 10% TCA to stop the reaction. Further, 0.75 mL of TBA reagent was added to tubes. The mixture was shaken and were heated in a water bath for 60 min at 95 °C and centrifuged at 10,000×g for 10 min. The pink color formed was measured at 532 nm after centrifugation of the tubes at 5000 rpm for 10 min [38]. Results were calculated as µM of MDA formed/mg protein.

### Statistical analysis

Statistical analysis of data are reported as mean±standard deviation using GraphPad Prism 4 software (GraphPad Software Inc., La Jolla, CA, USA). One-way ANOVA was used to compare the data, and the significant means were compared by

Duncan's multiple range test (DMRT). All statistical test with P < 0.05 were considered as significant.

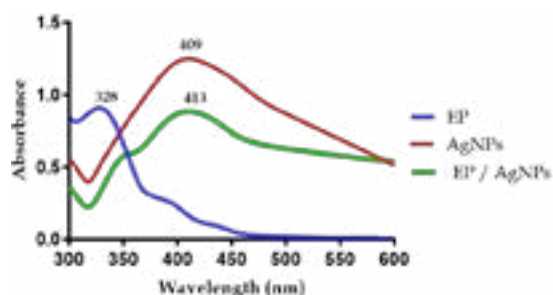


Fig 1. UV-visible absorption spectra of *E. polystachya* extract (EP), AgNPs and synthesized EP/AgNPs

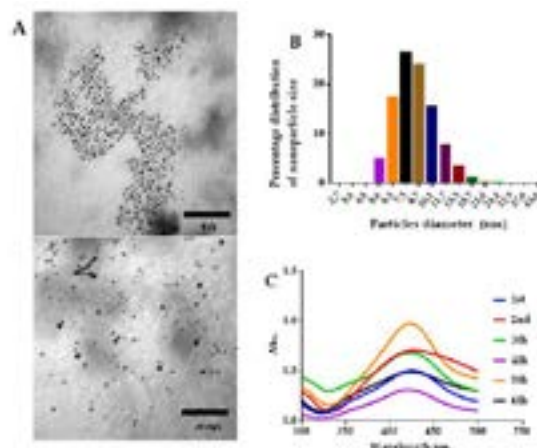


Fig 2. (A) TEM micrographs of silver nanoparticles prepared from *E. polystachya* extract EP; (B) Particle size distribution of silver particles; (C) UV-vis absorption spectra of the EP/AgNPs from 1 to 6 months

## RESULTS

### Characterization of EP-AgNPs by UV/vis absorption

The UV-vis spectra generated from the reduction of AgNO<sub>3</sub> to AgNPs using NaBH<sub>4</sub> show an absorption band at 409 nm. The absorption in this region depends on the wavelength of the surface plasmon resonance corresponding to the collective excitation of conduction electrons in the metal. In addition, this absorbance also confirmed the formation of AgNPs (Fig 1). Experimental observations indicate that the formation of a surface plasmon resonance band at 409 nm corresponds to the presence of spherical or roughly spherical nanoparticles. The UV-vis spectra also show a band at 413 nm, which supported the spherical-shaped EP/AgNPs with

approximately 5-20 nm in size. However, UV-vis spectra of EP extract two absorption peaks at 284 and 328 nm (Fig. 2) which are characteristic of the flavonoid bands I and II respectively, were perceived [39].

Table 1. Zeta potential, polydispersity index (PI), and hydrodynamic diameter of AgNPs synthesized with EP extract

Nanoparticles	Zeta potential mV	Polydispersity index	Hydrodynamic diameter nm
EP/AgNPs	-32.25	0.197	12

### TEM analysis of AgNPs

The information joined by the UV-vis spectra was complemented by TEM analysis. TEM images revealed that the AgNPs and EP/AgNPs are spherical in shape and polydispersed. The results indicate that nanoparticles did not form aggregates. The absence of agglomerated particles supported the stability of the nanoparticles. In addition, TEM analysis established that EP/AgNPs are in average diameter of 5.6-15.7 nm (Fig. 2A). Size distribution of the EP/AgNPs is presented in Fig 2B showing that the EP/AgNPs are in average particle size of  $12 \pm 0.15$  nm. Findings are in accordance with the result obtained from the UV-vis spectra.

### Studies of Zeta potential

Dynamic light scattering (DLS) analysis of EP/AgNPs was performed to measure the zeta potential value (Table 1). Zeta potential is an important assay to determine the stability of the EP/AgNPs coated with plant extract (EP). Finding, of Zeta potential of the EP/AgNPs was of -22.6 mV. The value negative zeta potential indicated that EP/AgNPs do not have agglomeration and are long-term stable supporting high dispersity and an appropriate colloidal nature as a consequence of negative-negative repulsion. Also, in Table 1 are shown the values of the hydrodynamic diameter (12 nm) and polydispersity index (PDI) of the EP/AgNPs (0.197). The high stability of nanoparticles is crucial for their applications in Zebrafish in this study.

### Stability of EP/AgNPs in aqueous solution

After, we was performed the stability studies for the biosynthesized EP/AgNPs in aqueous solution. UV-Vis spectra were recorded each 15 days. UV-Vis spectra showed similar surface plasmon resonance peaks for the EP/AgNPs dispersed in MilliQ water after 6 months (Fig 2C).

In consequence, the synthesized EP/AgNPs were exhibit to be high stable [40].

### FTIR analysis

FTIR analysis was used to identify the functional groups in nanoparticles in the capping of the reduced EP/AgNPs biosynthesized using EP extract. Some characteristic peaks of EP could be observed in FTIR spectra in Fig 3A. The strong band at  $3456 \text{ cm}^{-1}$  corresponded to O-H stretching vibrations of phenolic compounds. The band at  $2354 \text{ cm}^{-1}$  indicated to C-O vibrational stretching of carbonyl compounds. The strong peak at  $1512 \text{ cm}^{-1}$  corresponded with the  $\text{C}=\text{C}$  stretching vibration, and the bands at  $692 \text{ cm}^{-1}$ ,  $1370 \text{ cm}^{-1}$ , and  $1024 \text{ cm}^{-1}$ , corresponding to heterocyclic structures, as polyphenols and flavonoids. The peaks at  $1042 \text{ cm}^{-1}$  and  $1248 \text{ cm}^{-1}$  corresponding to the tension of the C-O of a methoxyl group ( $\text{O}-\text{Me}$ ). The bands clearly indicated the participation of polyphenols which are involved in the coating/capping around the nanoparticles. However, Fig. 3B shows the FT-IR spectra peaks produced by AgNPs biosynthesized with an EP extract.

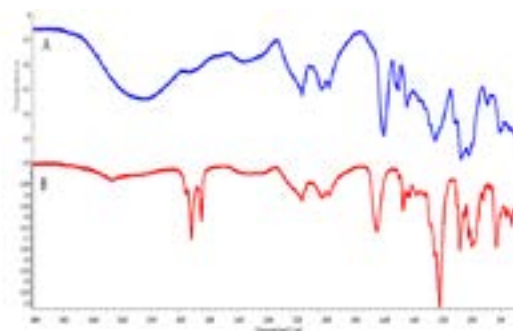


Fig 3. FT-IR spectra of EP/AgNP nanoparticles synthesized using chemical method; (A) EP; (B) EP/AgNP

### Loading efficiency and encapsulation efficiency

The encapsulation efficiency of a drug into a nanoparticle in a delivery system is one of the most important factors that should be considered. EP/AgNPs possessing a highest encapsulation efficiency of 80.8 % for EP with an incorporation efficiency of 44.34%. These data demonstrated that nanoparticles were effectively loaded.

### In vitro EP release profile

EP extract release profile from EP/AgNPs as a function of pH and the time are shown in Fig. 4A wherein showed the release profiles of EP for

2 hr at 37 °C and pH 1.2, in simulated immersion in gastric (SGF) a rapid release of 16.3% of the EP was observed. After of 10 h EP release remaining constant which can be due to the weak interaction between strongly anionic AgNPs and EP. Then was followed in simulated intestinal (SIF) fluid at pH 6.8 or pH 7.4 for 4 hr wherein the amount of EP was higher than that released at pH 1.2 following with a prolonged release of 75-88% maintained until 10 h which can be due to the interaction between the positive charges of the compounds contained in EP and alkaline medium. Finding, suggested that sustained releasing was regulated in a pH-dependent manner and the diffusion of EP through the system.

Table 2. Release constants from EP/AgNPs obtained from the Higuchi [29], Korsmeyer [30] and Ritger and Peppas [31] models

Nanoparticle	Model	Release constant	r <sup>2</sup>
EP/AgNPs	Higuchi	0.0089	0.949
	Korsmeyer	0.0003	0.853
	Ritger and Peppas	K <sub>1</sub> =1x10 <sup>-2</sup> K <sub>2</sub> =0.0009	0.973

#### Antioxidant assay against DPPH

We also determined the antioxidant effect of EP, for which the IC<sub>50</sub> value against DPPH was 38.21 µg/mL. In this study, the EP/AgNPs developed for their antioxidant properties showed an IC<sub>50</sub> value against DPPH of 36.7 µg/mL. The nanoparticles were effective in scavenging DPPH free radicals in the antioxidant assay for at least 70 h (Fig 4B). The antioxidant effect of the EP/AgNPs is maintained after a long-term storage since antioxidant compounds are slowly released from the nanoparticles.

#### The kinetics of release of EP

Table 2 shows the release kinetics of PE from EP/AgNPs. Results of the analysis based on the Korsmeyer-Peppas model the rate constant at the beginning of the release of EP was found to be 0.0003. The experimental data with the theoretical curve of Korsmeyer-Peppas [41, 42] model were presented in Fig 4C. The value of the release exponent r<sup>2</sup> was 0.853 indicating that EP transport mechanism was followed super case II transport [43]. Although the release kinetics shows a rapid release at the beginning of the assay followed by a controlled release is in accordance with the Higuchi model [44], The release profile of EP from AgNPs shows first-order kinetics [Fig 4D]. The phenolic compounds contained in EP are the

main responsible of the antioxidant effect [25].

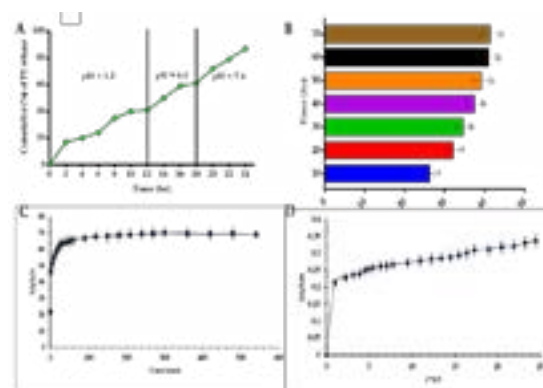


Fig 4. (A) (C) EP extract release profile from AgNPs as a function of pH and the time; (B) EP/AgNPs against DPPH free radical scavenging profile at different time periods; (C) Kinetics of EP release of EP/AgPANP ; (D) Behavior of nanoparticles using the Higuchi model. (Mt = concentration of EP in time and Mo = concentration of theoretical EP). Data represent the mean ± SD of three independent experiments. aP<0.05, bP<0.001

#### Biocompatibility of EP/AgNPs

This study also evaluated as EP/AgNPs affect cell viability in RAW264.7 murin macrophages cells using the MTT method. Date indicated that at a concentration of 560 µg/mL was higher than 90% viability observed after 24 h exposure of the macrophages to EP/AgNPs supporting the biocompatibility of the nanoparticles (Fig 5).

#### Mortality

For the assessment of toxicity of nanoparticles, different concentrations of EP/AgNPs (25 and 200 mg/mL) was added. Control group without EP/AgNPs was monitored simultaneously. The survival rate of Zebrafish with EP/AgNPs exposed to concentrations 25 and 200 mg/mL were 96.12% and 92.70% respectively; these data are not significantly different (P<0.05) from the values obtained for the control group. Mortality of Zebrafish in the control and EP/AgNPs groups exposed were not observed confirmed biocompatibility of EP/AgNPs.

#### Protective effect of EP/AgNPs against glucose-induced oxidative stress in zebrafish embryos/larva

The first line of cellular defense against oxidative stress consists of antioxidant enzymes such as CAT, SOD and GPx. Therefore, antioxidant defense plays an important role in the protection

Table 3. Changes produced by EP and EP/AgNPs in expression of total protein, CAT SOD, GPx and MDA in zebrafish embryos with diabetes induced-glucose Zebrafish embryos with diabetes induced-glucose were exposed to 25, 50, 100 and 200 mg/L of EP/AgNPs, 200 mg/L of EP and 5 mg/L de glibenclamide (GB) as standard. Values are shown as means standard deviation of triplicate samples. abcMean values within a row not sharing the same superscript letters were significantly different, a p< 0.01 vs diabetic control, bp < 0.05 vs normal control, cp < 0.05 vs GB by the Newman-Keuls posthoc multiple comparisons test

Treatments	Total protein (mg)	CAT activity (U/mg Protein)	SOD activity (U/mg Protein)	GPx activity (U/mg Protein)	MDA Content (nmol/mg Protein)
NC	0.321±0.054	0.433±0.035	199.3±3.7	1.11±0.05	0.167±0.015
Diabetic control	0.265±0.012 <sup>bc</sup>	0.145±0.024 <sup>bc</sup>	57.7±6.6 <sup>bc</sup>	0.82±0.09 <sup>bc</sup>	0.227±0.005 <sup>bc</sup>
PA (200 mg/L)	0.348±0.007 <sup>a</sup>	0.383±0.05 <sup>ab</sup>	160.7±16.3 <sup>abc</sup>	0.92±0.14 <sup>ab</sup>	0.190±0.009 <sup>ab</sup>
EP/AgNP (25 mg/L)	0.341±0.008 <sup>a</sup>	0.319±0.064 <sup>ab</sup>	160.3±16.4 <sup>abc</sup>	0.84±0.12 <sup>abc</sup>	0.222±0.010 <sup>bc</sup>
EP/AgNP (50 mg/L)	0.312±0.031 <sup>a</sup>	0.348±0.051 <sup>ab</sup>	177.7±10.7 <sup>a</sup>	0.86±0.23 <sup>abc</sup>	0.214±0.013 <sup>bc</sup>
EP/AgNP (100 mg/L)	0.319±0.104 <sup>a</sup>	0.379±0.149 <sup>ab</sup>	183.8±8.5 <sup>a</sup>	0.90±0.16 <sup>ab</sup>	0.206±0.005 <sup>abc</sup>
EP/AgNP (200 mg/L)	0.302±0.008 <sup>a</sup>	0.410±0.052 <sup>a</sup>	191.3±13.7 <sup>a</sup>	0.96±0.02 <sup>ab</sup>	0.189±0.003 <sup>ab</sup>
GB (5 mg/L)	0.325±0.012 <sup>a</sup>	0.409±0.017 <sup>a</sup>	170.8±11.9 <sup>ab</sup>	0.96±0.11 <sup>ab</sup>	0.185±0.009 <sup>ab</sup>

of cells against oxidative stress. Induction of oxidative stress by glucose in zebrafish embryos/larvae caused a marked reduction in the levels of these enzymes.

Total protein levels were significantly ( $P<0.05$ ) suppressed in the embryos that received glucose treatment. In embryos treated with EP and EP/AgNPs for 96 h, total protein was increased compared to the diabetic control (Table 3). A significant ( $P<0.05$ ) activation of CAT, SOD, and GPx compared with the diabetic control group was observed after 96 h of administration of EP and EP/AgNPs at 200 mg/L. The level of activity of the antioxidant enzymes is shown in Table 3. The levels of lipid peroxidation based on malondialdehyde (MDA) content were evaluated in all EP/AgNPs-treated groups as a measure of the oxidative stress induced by glucose (Table 3). The MDA level showed an increase at 96 h, but a significant ( $P<0.05$ ) decrease in MDA was observed in the EP- and EP/AgNPs-treated groups after 96 h exposure; thus, the MDA level was significantly reversed in the treated group compared to the diabetic group. Zebrafish embryos/larvae treated with glibenclamide (5 mg/L) showed increased levels of antioxidant enzymes, and total protein levels and decreased malondialdehyde compared to the diabetic control group, with values similar to those presented by embryos and larvae exposed to EP/AgNPs.

## DISCUSSION

The nanoparticles synthesized from EP have sustained drug release ability and are

biocompatible and nontoxic in nature. The two factors size distribution and size of EP/AgNPs play an important role in the measure of EP release and stability. Nanoparticles synthesized with the herbal extract from *Eysenhardtia polystachya*, [45] obtaining spherical or semi-spherical shape nanoparticles ranging in size between 0.5 and 100 nm [27] corresponding to the data found in other studies. This kind of nanoparticles are used as a nanotransportation system, for the administration of biomolecules such as phenols, flavonoids, terpenes, terpenoids, polysaccharides, alginates, flavones, chalcones, chlorophylls, carotenoids, etc., and have shown to reduce oxidative stress, and free radicals, and therefore are useful to treat of type 2 diabetes [46, 47]. The bioactive flavonoids found in the bark of *E. polystachya* have been previously identified; these are similar to flavonoids isolated of other plants with antidiabetic effect [48].

The zeta potential value for EP/AgNPs was -22.6 mV, which suggest that the nanoparticles were well dispersed and sufficiently stable. However, the negative zeta potential value may be due to capping agents, which mainly consisted of negatively charged groups coating the surface of EP/AgNPs. The diameter of the EP/AgNPs was 12 nm, in accordance with other studies of AgNPs synthesized using plant extracts with a hydrodynamic diameters value range to 10 to 100 nm [49, 50]. The stability of the EP/AgNPs was confirmed with the polydispersity index value of 0.197 in accordance with the values of other AgNPs synthesized from plant extracts [51]. The

stability of the EP/AgNPs was supported for the absence of aggregation of nanoparticles after six months of storage.

The FT-IR spectrum provides information on the identity of the types of biomolecules that determine the nanoparticles functionality. FTIR analysis was used to characterize potent biomolecules of *E. polystachya* with silver nanoparticles. Conformable to the FTIR spectra of EP/AgNPs different bands were obtained indicating intermolecular bonding of nanoparticles and different functional groups. The functional groups in FTIR spectra are from heterocyclic substances that are polyphenol compounds of *E. polystachya* that are capable of capping ligands for the formation of nanoparticles (52, 53). Also, these compounds are capable to stabilizing and reduced the agglomeration of nanoparticles during synthesis (54).

Finding, indicate that the method used to produced nanoparticles of spherical and semi-spherical shape was adequate, obtaining results comparable to others nanoparticles synthesized with herbal extracts [49, 50]. Many plant have bioactive compounds which have been assayed in clinical trials, likewise in the present study measured effect of EP/AgNPs biologically synthesized from *E. polystachya* bark extract in treating diabetes zebrafish.

Oxidative stress, is one of the main factors in diabetes that lead to  $\beta$ -cell destruction, generating impairment of antioxidant defence mechanism leading to damage in the  $\beta$ -cells. While, the antioxidants contain in plants be able to revert these harmful changes. The main role of SOD is catalyze the dismutation of the superoxide anion radical ( $O_2^{\cdot-}$ ) into  $H_2O_2$  and water, then CAT reduce its to  $H_2O$  and oxygen for the removal of ROS (55). GPx scavenge residual free radicals produced from oxidative metabolism [55]. Lipid peroxidation, is an important factor of the oxidative stress, being the main cause of the loss of cell performance under oxidative stress (56). The level of MDA content (as index of LPO) establish a relative potential effect of glucose in Zebrafish to produce oxidative damage since MDA is the final product of lipid peroxidation and their levels indicate the toxicity produced by free radicals. The results suggest that the increase of LPO has been widely used as a biomarker in the evaluation of eco-toxicological test for indicate oxidative stress. The CAT and SOD system are also

used as biomarkers because are the first line of defense against oxygen toxicity [57].

Importants alterations were observed in the glutathione peroxidase (GPx), catalase (CAT) and superoxide dismutase (SOD) level and malondialdehyde (MDA) and lipid peroxidation (LPO) contents in zebrafish exposed to glucose at concentration of 25 mM/L. The Zebrafish exposed to glucose showed that MDA and LPO levels were found to be markedly high when compared with the control. Also finding, indicated a significant reduction in the activity of SOD, GPx, and CAT compared to the control. However, induced diabetic embryos exposed to EP/AgNPs has been found increase activities of the protein expression of GPx, SOD and CAT. Also decrease MDA and LPO levels which may be due to the excess ROS production is inactivated avoiding excessive ROS accumulation and improved tissue injury.

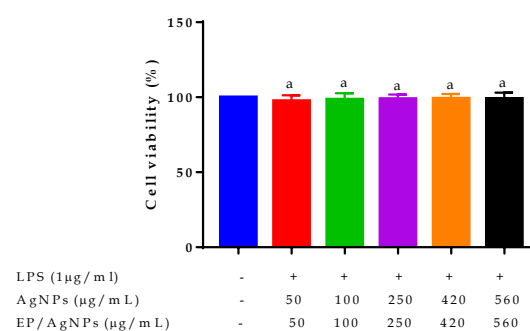


Fig 5. Effect of EP/AgNPs (50, 100, 250, 420 and 560 µg/ml) on the viability of RAW264.7 cells. Data represent the mean  $\pm$  SD of three independent experiments. Compared with LPS group aP<0.05

## CONCLUSIONS

Oxidative stress induce changes in antioxidant responses, including alterations of total protein content CAT, SOD, GPx activities, as well as LPO damage, which was observed in the *D. rerio* embryos. MDA was increased in zebrafish embryos exposed to glucose. EP and EP/AgNPs showed a significantly ( $P<0.05$ ) increase on antioxidant enzyme activities including CAT, SOD, and GPx. It can be inferred that the antioxidant defense in zebrafish exposed to glucose was overwhelmed; as a consequence of the free radical production that exceed the scavenging capability of cells and its antioxidants mechanisms, leading to increased MDA levels. EP and EP/AgNPs restored the enzymatic antioxidant system that was able to reduce ROS production, decreasing the generation

of MDA. The present study reveals that EP/AgNPs demonstrated significantly antidiabetic activity.

## REFERENCES

- Valko M, Rhodes J, Moncol J, Izakovic M, Mazur M. Free radicals, metals and antioxidants in oxidative stress-induced cancer. *Chem Biol Interact.* 2006; 160(1): 1–40.
- Rahman T, Hosen I, Towhidul MM, Shekha HU. Oxidative stress and human health. *Adv Biosc Biotech.* 2012; 3: 997–1019.
- Dobrakowski M, Boroń M, Birkner E, Kasperczyk A, Chwalińska E, Lisowska G, Kasperczyk S. The effect of a short-term exposure to lead on the levels of essential metal ions, selected proteins related to them, and oxidative stress parameters in humans. *Oxid Med Cell Longev.* 2017; 2017: 8763793.
- Birben E, Sahiner UM, Sackesen C, Erzurum S, Kalayci O. Oxidative stress and antioxidant defense. *World Allergy Organ J.* 2012; 5(1): 9–19.
- Kayalvizhi T, Ravikumar S, Venkatachalam P. Green synthesis of metallic silver nanoparticles using *Curculigo orchioides* rhizome extracts and evaluation of its antibacterial, larvicidal, and anticancer activity. *J Environ Eng.* 2016; 142: (144) C4016002.
- Marin S, Vlasceanu GM, Tiplea RE, Bucur IR, Lemnaru M, Marin MM, Grumezescu AM. Applications and toxicity of silver nanoparticles: A recent review. *Curr Top Med Chem.* 2015; 15(16): 1596–604.
- Gurunathan S, Raman J, Abd Malek SN, John PA, Vikineswary S. Green synthesis of silver nanoparticles using *Ganoderma neojaponicum* Imazeki: a potential cytotoxic agent against breast cancer cells. *Int J Nanomed.* 2013; 8: 4399–4413.
- Kim JS, Kuk E, Yu KN, Kim JH, Park SJ, Lee HJ. Antimicrobial effects of silver nanoparticles. *Nanomed Nanotechnol.* 2007; 3(1): 95–101.
- Emerich DF, Thanos CG. The pinpoint promise of nanoparticle-based drug delivery and molecular diagnosis. *Biomol Eng.* 2006; 23(4): 171–184.
- Froeschke S, Kohler S, Weber AP, Kasper G. Impact fragmentation of nanoparticle agglomerates. *Aerosol Sci.* 2003; 34(3): 275–287.
- Mandal S, Sainkar SR, Sastry M. Attended silver nanoparticles films by an ion complexation process in thermally evaporated fatty acid films. *Mater Res Bull.* 2002; 37(1): 1613–1621.
- Marzan LML, Tourino I L. Reduction and stabilization of silver nanoparticles in ethanol by nonionic surfactants. *Langmuir.* 1996; 12: 3585–3589.
- Petit C, Lixon P, Pileni MP. In situ synthesis of silver nanoclusters in AOT reverse micelles. *J Phys Chem.* 1993; 97: 12974–12983.
- Zahran M, El-Kemary M, Khalifa S, El-Seedi H. Spectral studies of silver nanoparticles biosynthesized by *Origanum majorana*. *Green Process Synth* 2017; 7(2): 5–10.
- Gholamreza A, Varshosaz J, Shahbaz N. Synthesis of silver nanoparticle using *Portulaca oleracea* L. extracts. *Nanomed J.* 2014; 1(2): 94–99.
- Sahu K, Gupta PK. Review on *Bauhinia variegata* linn. *Int Res J Pharm.* 2012; 3(3): 48–51.
- Lila MA. Anthocyanins and human health: an in vitro investigative approach. *J Biomed Biotechnol.* 2004; 2004: 306–313.
- El-Kemary M, Zahran M, Khalifa SAM, El-Seedi, HR. Spectral characterisation of the silver nanoparticles biosynthesised using *Ambrosia maritima* plant. *Micro Nano Lett.* 2016; 11(1):311–314.
- McShan D, Paresh CR, Yu H. Molecular toxicity mechanism of nanosilver. *J Food Drug Anal.* 2014; 22(1): 116–117
- Fishman MC. Zebrafish genetics: the enigma of arrival. *Proc Natl Acad Sci U S A.* 1999; 96(19): 10554–56.
- Perez RMG, Vargas R, Perez GS, Zavala S. Antiuroliithiatic activity of *Eysenhardtia polystachya* aqueous extract on rats. *Phytoter Res.* 1998; 12: 144–45.
- Burns DT, Dalgarno BG, Gargan P, Grimshaw J. An isoflavone and a coumestan from *Eysenhardtia polystachya* Robert boyles fluorescent acid-base indicator. *Phytochemistry* 1984; 3(1): 167–169.
- Alvarez L, Rios MY, Esquivel C, Chavez MI, Delgado G, Aguilar G. Cytotoxic isoflavans from *Eysenhardtia polystachya*. *J Nat Prod.* 1999; 61(6): 767–770.
- Perez RMG, Baez EG. Evaluation hypoglycemic, antioxidant and antiglycating activities of the *Eysenhardtia polystachya*. *Pharmacog Mag* 2014; (Supplement 2)10: S404–S418.
- Perez RMG, Campoy AHG, Ramirez AM. Properties of flavonoids isolated from the bark of *Eysenhardtia polystachya*, and their effect on oxidative stress in streptozotocin-induced diabetes mellitus in mice. *Oxid Med Cell Longev.* 2016; 2016: 9156510.
- Perez RMG, Campoy AHG, Flores JMM. Dihydrochalcones from the bark of *Eysenhardtia polystachya* inhibit formation of advanced glycation and products at multiple stages in vitro studies. *J Pharm Pharmacol.* 2017; 1(3): 3–23.
- Hang L, Zhao J, Chen J, Zhu L, Wang D, Jiang L, Yand D, Zhao Z. Diterpenoids from aerial part of *Flickingeria fimbriata* and their nuclear factor-kappaB inhibitory activities. *Phytochemistry.* 2015; 117: 400–409.
- Ahmed SI, Ahmad MI, Swami BLI, kram SI. A review on plants extract mediated synthesis of silver nanoparticles for antimicrobial applications: A green expertise. *J Adv Res.* 2016; 7(1): 17–28.
- Lee JH, Ki J. Effect of cubic phase nanoparticle on obesity-suppressing efficacy of herbal extracts. *Biotechnol Bioprocess Engin.* 2015; 20: 1005–1015.
- Nayak D, Minz AP, Ashe S, Rauta PR, Kumari M, Chopra P, Nayak B. Synergistic combination of antioxidants, silver nanoparticles and chitosan in a nanoparticle based formulation: Characterization and cytotoxic effect on MCF-7 breast cancer cell lines. *J Colloid Interface Sci.* 2016; 470: 142–152.
- Nasiriboroumand M, Montazer M, Barani H. Preparation and characterization of biocompatible silver nanoparticles using pomegranate peel extract. *J Photochem Photobiol B.* 2018; 179: 98–104.
- Saravanakumar K, Wang MH. Trichoderma based synthesis of anti-pathogenic silver nanoparticles and their characterization, antioxidant and cytotoxicity properties. *Microb Pathog.* 2017; 114: 269–273.
- Suvakanta D, Padala NM, Lakanta Prasanta C. Kinetic modeling on drug release from controlled drug delivery systems. *Acta Poloniae Pharm- Drug Res.* 2010; 67(3): 217–23.
- Hu R, Bai H, Liu F, Wu Y, XIE X, Hu L. Anti-proliferative and apoptotic effects of S1, a tetrandrine derivative, in

- human gastric cancer BGC-823 cells. *Chin J Nat Med*. 2016; 14(7):527-533.
35. Gleeson M, Connaughton V, Arneson S. Induction of hyperglycaemia in zebrafish (*Danio rerio*) leads to morphological changes in the retina. *Acta Diabetol*. 2007; 44(4): 157-163.
  36. Mugoni V, Camporeale A, Santoro MM. Analysis of oxidative stress in zebrafish embryos. *J Vis Exp*. 2014; (89): e51328.
  37. Bradford MM. A rapid and sensitive for the quantitation of microgram quantities of protein utilizing the principle of protein-dye binding. *Anal Biochem*. 1976; 72: 248-254.
  38. Ohkawa H, Ohishi N, Yagi K. Assay for lipid peroxides in animal tissues by thiobarbituric acid reaction. *Anal Biochem*. 1979; 95: 351-358.
  39. Maybry TJ, Markham KR, Thomas MB. The ultraviolet spectra of flavones and flavonols. The systematic identification of flavonoids. Springer Berlin Heidelberg. 1970; 41-164.
  40. Velgoso O, Mrazikova A. Limitations and possibilities of green synthesis and long-term stability of colloidal Ag nanoparticles. 2017; AIP Conference Proceedings 1918, 020004.
  41. Dash S, Murthy PN, Nath L, Chowdhury P. Kinetic modeling on drug release from controlled drug delivery systems. *Acta Pol Pharm Drug Res*. 2010; 67(3): 217-223.
  42. Higuchi T. Mechanism of sustained-action medication. Theoretical analysis of rate of release of solid drug dispersed in solid matrices. *J Pharm Sci*. 1963; 52 (12): 1145-1149.
  43. Korsmeyer RW, Gurny R, Doelker EM, Buri P, Peppas NA. Mechanism of release from porous hydrophilic polymers. *Int J Pharm*. 1983; 15 (1): 25-35.
  44. Ritger P, Peppas N. A simple equation for description of solute release I. Fickian and non-Fickian release from non-swelling device in the form of slabs, spheres, cylinders or discs. *J Control Release*. 1987; 5 (1): 23-26.
  45. Logeswari P, Silambarasan S, Abraham J. Synthesis of silver nanoparticles using plants extract and analysis of their antimicrobial property. *J Saudi Chem Soc*. 2015; 19(3): 311-317.
  46. Kim JY, Hong JH, Jung HK, Jeong YS, Cho KH. Grape skin and loquat leaf extracts and acai puree have potent anti-atherosclerotic and anti-diabetic activity in vitro and in vivo in hypercholesterolemic zebrafish. *Int J Mol Med*. 2012; 30(3): 606- 614.
  47. Perez-Gutierrez RM. Review: The potential of chalcones as a source of drugs. *African J Pharm Pharma*. 2015; 9(34): 861-874.
  48. Kuppasamy P Yusoff MM, Maniam GP, Govindan N. Biosynthesis of metallic nanoparticles using plant derivatives and their new avenues in pharmacological applications – An updated report. *Saudi Pharm J*. 2016; 24(4): 473-484.
  49. Kayalvizhi K, Ravikumar S, Venkatachalam P. Green synthesis of metallic silver nanoparticles using *Curculigo orchioides* rhizome extracts and evaluation of its antibacterial, larvicidal, and anticancer activity. *J Environ Eng*. 2016; 142(9): C4016002.
  50. Dipankar C, Murugan S. The green synthesis, characterization and evaluation of the biological activities of silver nanoparticles synthesized from *Iresine herbstii* leaf aqueous extracts. *Coll Surf B Biointerfaces* 2012; 98(4): 112-119.
  51. Johnson P, Krishnan V, Loganathan C, Govindhan K, Raji V, Sakayanathan P, Vijayan S, Sathishkumar P, Palvannan T. Rapid biosynthesis of *Bauhinia variegata* flower extract mediated silver nanoparticles: an effective antioxidant scavenger and  $\alpha$ -amylase inhibitor. *Artificial Cells Nanomed Biotech*. 2017; Epub ahead of print.
  52. El-Kemary M, Zahran M, Khalifa SAM, the Silver nanoparticles biosynthesized using *Ambrosia maritima* plant. *Micro and Nano Letters*. (2016). 11(6): 311-314.
  53. Patil Shrinivas P, Kumbhar Subhash T. Antioxidant, antibacterial and cytotoxic potential of silver nanoparticles synthesized using terpenes rich extract of *Lantana camara* L. leaves. *Biochem Biophys Report*. 2017; 10: 76-81.
  54. Geetha N, Geetha TS, Manonmani P, Thiyagarajan M. Green synthesis of silver nanoparticles using *Cymbopogon citratus* (DC) Stapf. Extract and Its Antibacterial Activity. *Australian J Basic and App Sci*. 2014; 8(3): 324-331.
  55. Halliwell B, Gutteridge JMC. Free radicals Press, Oxford. 2015; <https://doi.org/10.1093/acprof:oso/9780198717478.001.0001>.
  56. Afifi M, Saddick S, Abu Zinada OA. Toxicity of silver nanoparticles on the brain of *Oreochromis niloticus* and *Tilapia zillii*. *Saudi J Biol Sci*. 2016; 23(6): 754-760.
  57. Pandey S, Parvez S, Sayeed I, Haque R, Bin-Hafeez B, Raisuddin S. Biomarkers of oxidative stress: a comparative study of river Yamuna fish *Wallago attu* (Bl. & Schn.). *Sci Total Environ*. 2003; 309(1-3): 105-115.